

Design considerations and analytical approximations for high continuous-wave power, broad-waveguide diode lasers

D. Botez^{a)}

Reed Center for Photonics, University of Wisconsin–Madison, Madison, Wisconsin 53706

(Received 8 January 1999; accepted for publication 29 March 1999)

Accurate analytical approximations are derived for the equivalent transverse spot size, d/Γ (<5% error), and the transverse beamwidth $\theta_{1/2}$ (<2% error), of broad-waveguide-type diode lasers, over a wide range in waveguide width: from the first-order-mode cutoff to the third-order-mode cutoff. The analytical formulas are found to be in good agreement with experimental values. For low-series-resistance and thermal-resistance devices, it is found that the junction-temperature rise ΔT_j in continuous wave (CW) operation is a strong function of both the characteristic temperature T_1 for the external differential quantum efficiency η_D as well as of the heatsink thermal resistance. If the device has relatively temperature-insensitive η_D (i.e., $T_1 \geq 1000$ K) the maximum CW power as well as the power density at catastrophic optical mirror damage, \bar{P}_{COMD} , are limited, for a given active-region material, only by the heatsink heat-removal ability. For large d/Γ , $0.97 \mu\text{m}$ emitting, $100 \mu\text{m}$ stripe InGaAs/InGaAs(P)/GaAs devices with $T_1 = 1800$ K, record-high CW and quasi-CW ($100 \mu\text{s}$ wide pulses) output powers are obtained. The ratio of quasi-CW to CW \bar{P}_{COMD} values is only 1.3, in contrast to devices of poor carrier confinement and subsequent low- T_1 values (~ 140 K), for which the ratio is 1.9, and whose maximum CW powers are $\sim 40\%$ less than those obtainable from high- T_1 devices. © 1999 American Institute of Physics. [S0003-6951(99)03421-X]

In the quest for high continuous-wave (CW) powers from diode lasers, one key concept has been that of the broad-waveguide (BW) separate-confinement heterostructure (SCH);^{1,2} that is, a structure that concomitantly provides both a large equivalent (transverse) spot size³ as well as low internal cavity loss,¹⁻³ α_i ($\leq 1 \text{ cm}^{-1}$) with no sacrifice in wall-plug efficiency at high drive levels.⁴ As a result, record-high CW powers have been achieved from BW-type devices at wavelengths from the visible to the midinfrared.⁴⁻⁹

Here, we derive for BW-type devices accurate analytical expressions for the equivalent spot size, d/Γ [d is quantum-well(s) thickness and Γ the (transverse) optical-confinement factor] and the transverse beamwidth. In addition, we compare record-high CW and quasi-CW (QCW) data at $\lambda = 0.97 \mu\text{m}$ and determine which parameters are critical for achieving high CW power at catastrophic optical mirror damage (COMD).

From the definition⁷ of the internal optical-power density at COMD, \bar{P}_{COMD} , one can express the maximum CW power as

$$P_{\text{max,cw}} = \left(\frac{d}{\Gamma}\right) W \left(\frac{1-R}{1+R}\right) \bar{P}_{\text{COMD}}, \quad (1)$$

where W is the stripe width and R the front-facet reflectivity. It has been established that for conventionally facet-passivated diodes \bar{P}_{COMD} is a function of the active-region material,¹⁰ being in effect inversely proportional¹¹ to the surface-recombination velocity s as long as¹² $s \geq 10^5 \text{ cm/s}$. That is, for a given active-region material with $s \geq 10^5 \text{ cm/s}$ and given stripe width, $P_{\text{max,cw}}$ directly scales with d/Γ . One main way to increase d/Γ is to use BW-SCH structures.³

A schematic representation of the BW-SCH laser structure and its optical-mode profile is shown in Fig. 1. Since the quantum-well(s) width d is much smaller than the waveguide width t_c , the optical-mode profile is primarily determined by the waveguide index profile. The normalized waveguide thickness D is defined as^{13,14}

$$D = \frac{2\pi}{\lambda} t_c \sqrt{n_w^2 - n_{\text{cl}}^2}, \quad (2)$$

where n_w, n_{cl} are the waveguide-layer and cladding-layer indices; and λ is the vacuum wavelength. Since the waveguide is large ($t_c > 0.5 \mu\text{m}$), D takes values in excess of 3, thus providing optical-mode intensity profiles excellently approximated by Gaussian curves.^{4,13} Then, considering the expression for a normalized Gaussian curve¹⁴ of waist w , one can easily find the fraction of power $\delta P/P$ confined to a small interval δx at the center of the curve:

$$\frac{\delta P}{P} = \delta x/w \sqrt{\pi/2}. \quad (3)$$

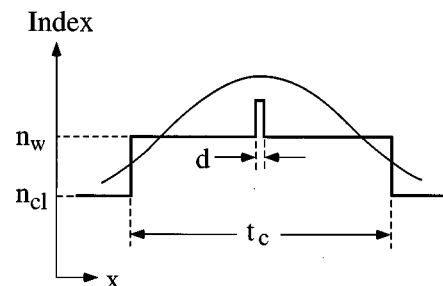


FIG. 1. Schematic representation of BW-type laser structure: effective-index profile and field-intensity profile. d is the (total) quantum-well(s) thickness and t_c is the waveguide width.

^{a)}Electronic mail: botez@engr.wisc.edu

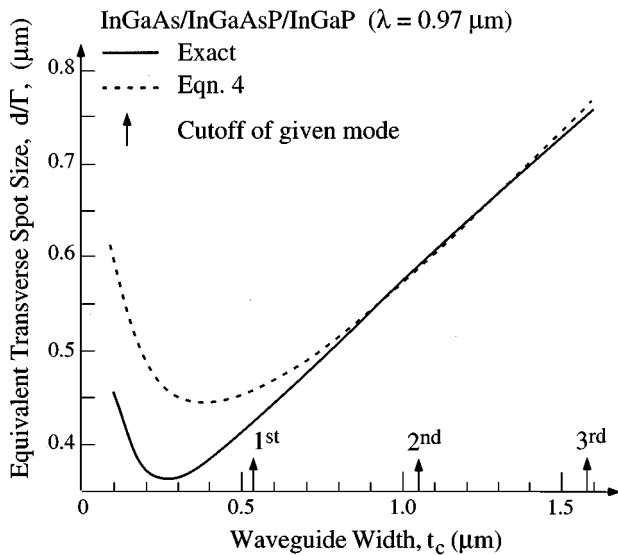


FIG. 2. The equivalent transverse spot size d/Γ vs the waveguide width for a InGaAs/InGaAsP/InGaP BW structure (Refs. 3 and 4) ($\lambda = 0.97 \mu\text{m}$). Solid curve: exact calculation. Dashed curve: approximation [Eq. (4)]. Arrows indicate the cutoff thickness for the first-, second-, and third-order modes.

Since for a BW-type device the quantum well(s) are very narrow compared to the waveguide, one can consider that the interval δx can be replaced by the (total) quantum-well(s) thickness d ; and, since the field is virtually uniform across the quantum well(s), $\delta P/P = \Gamma$. Then, by using a previously derived¹⁴ accurate analytic approximation for w we obtain:

$$\frac{d}{\Gamma} \approx \sqrt{\frac{\pi}{2}} w = \sqrt{\frac{\pi}{2}} t_c (0.31 + 2.1/D^{3/2}), \quad \pi < D < 3\pi. \quad (4)$$

Figure 2 shows a comparison of d/Γ curves: exact calculation and the analytical approximation (4); for a InGaAs/InGaAs(P)GaAs structure^{3,4} at $\lambda = 0.97 \mu\text{m}$. It is evident that for $t_c > 0.53 \mu\text{m}$ (i.e., the first-order-mode cutoff; $D = \pi$) the approximation has errors $< 5\%$ up to $t_c = 1.60 \mu\text{m}$, the third-order-mode cutoff ($D = 3\pi$). Most BW-SCH structures are designed near the second-order-mode cutoff ($t_c \approx 1.0 \mu\text{m}$), where the d/Γ approximation is extremely accurate ($< 1\%$ error). The approximation is also excellent ($< 1\%$ error) up to the third-order-mode cutoff, a fact relevant to BW devices for which the second-order mode is suppressed via transverse losses.⁴

Equation (4) makes it clear that for large waveguides ($t_c \geq 1.0 \mu\text{m}$) d/Γ is basically proportional to t_c . Furthermore, rearranging Eq. (4) provides an accurate analytical approximation for Γ of BW-SCH devices, which in turn can be used in the threshold-current-density expression.

Now one can find an analytical expression for $\theta_{1/2}$, the beam full width at half maximum:

$$\theta_{1/2} \approx 1.18 \tan^{-1}(\lambda/\pi w_o), \quad (5)$$

$$w_o = t_c (0.31 + 2.2/D^{3/2} + 30/D^6),$$

where w_o is the equivalent near-field Gaussian waist.¹⁵ Equation (5) is obtained from previous work¹⁵ as well as from curve fitting in Fig. 3. As seen from Fig. 3, the approximation applied at $\lambda = 0.97 \mu\text{m}$ to InGaAs/InGaAsP/InGaP devices⁴ is very accurate ($\leq 2\%$ error) for $t_c \geq 0.5 \mu\text{m}$ (i.e.,

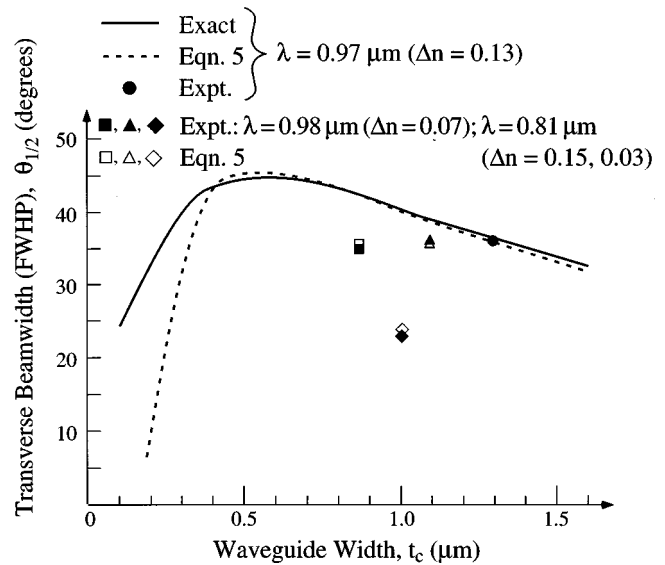


FIG. 3. The transverse beam full width at half maximum $\theta_{1/2}$ for a InGaAs/InGaAsP/InGaP BW structure (Refs. 3 and 4) ($\lambda = 0.97 \mu\text{m}$). Solid curve: exact calculation. Dashed curve: Gaussian approximation [Eq. (5)]. Solid and open symbols correspond to experimental and approximated $\theta_{1/2}$ values for BW lasers emitting at $\lambda = 0.97 \mu\text{m}$ (Ref. 4), $\lambda = 0.98 \mu\text{m}$ (Ref. 16), and $\lambda = 0.81 \mu\text{m}$ (Refs. 7 and 17).

$D \geq \pi$); that is, for the Gaussian-like field regime. Comparing to experimental results from BW lasers,^{4,7,16,17} we find good agreement with values given by Eq. (5). It is evident that increasing t_c will decrease $\theta_{1/2}$. However, an even more important factor for lowering $\theta_{1/2}$ is to decrease the index step, $\Delta n = n_w - n_{cl}$, as amply demonstrated for InGaAsP/AlGaAs devices.¹⁷

Equation (1) gives the maximum CW power, provided that junction-heating effects do not cause power saturation. Figure 4 shows the CW and QCW (100 μs wide pulses) light-current characteristics for 100 μm stripe, 2 mm long InGaAs/InGaAsP/InGaP 0.97 μm diode lasers mounted on Cu heatsinks.^{18,19} Maximum power levels in CW and QCW operation are 11 and 14.3 W, respectively, and limited by COMD.

Considering a d/Γ value⁴ of $0.66 \mu\text{m}$, \bar{P}_{COMD} is 18 and

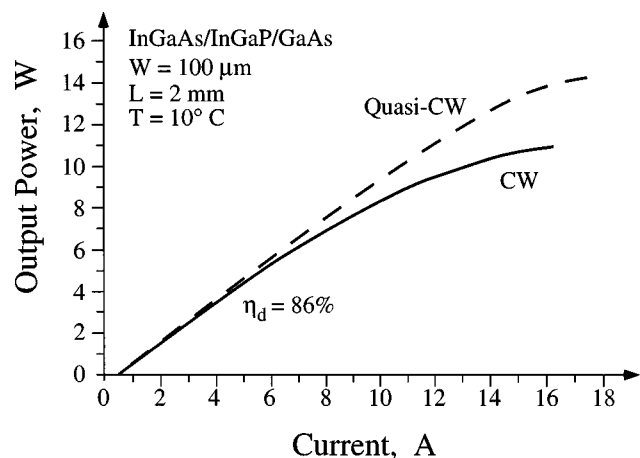


FIG. 4. CW and quasi-CW (100 μs wide pulses) light-current characteristics for lasers employing the BW structure described in Ref. 4 ($\lambda = 0.97 \mu\text{m}$). The devices are mounted on Cu heatsinks, and the front- and back-facet reflectivities are 3% and 95%. η_d is the differential quantum efficiency.

23 MW/cm² in CW and QCW operation, respectively. The QCW \bar{P}_{COMD} is basically the same as for InGaAs/GaAs/InGaP 0.99 μm emitting devices with the same 100 μm wide aperture,²⁰ but there is a big discrepancy between the ratio of QCW \bar{P}_{COMD} to CW \bar{P}_{COMD} . That is, for the device with a high-band-gap waveguide layer [i.e., InGaAsP (1.62 eV)] shown in Fig. 4, the ratio is 1.3, while for devices with a low-band-gap waveguide layer [i.e., GaAs (1.42 eV)],²⁰ the ratio is 1.9. To understand this dramatic difference one has to look at the junction-temperature rise ΔT_j in CW operation:

$$\Delta T_j = R_{\text{th}}(IV - P_{\text{opt}}), \quad (6)$$

where R_{th} is the thermal resistance, IV is the current-voltage product, and P_{opt} is the emitted optical power. V is the sum of an overall built-in voltage²¹ V_o and IR_s , where R_s is the series resistance. If R_s is small, as is the case for Al-free BW devices,^{4,20} it is clear from Eq. (6) that ΔT_j is mainly a strong function of R_{th} as well as of P_{opt} .

P_{opt} is a function of temperature since both the threshold current I_{th} , as well as the external differential quantum efficiency η_D , are temperature sensitive, characterized^{4,22} by the coefficients T_0 and T_1 , respectively,

$$P_{\text{opt}}(T) = \eta_D(T) V_c [I - I_{\text{th}}(T)], \quad (7a)$$

and at high drives (i.e., $I > 10I_{\text{th}}$),

$$P_{\text{opt}}(T) \approx \eta_D(T) V_c I \approx \eta_D(T_h) \exp\left(-\frac{\Delta T_j}{T_1}\right) V_c I, \quad (7b)$$

where V_c is $h\nu/q$; and T_h is the heatsink temperature ($T = T_h + \Delta T_j$). Therefore, the temperature dependence of P_{opt} at high drive levels is primarily determined by the temperature dependence of η_D . The coefficient T_1 gives the temperature sensitivity of η_D (Ref. 22) (in pulsed operation) from threshold to $\sim 20 \times$ threshold. For these devices, due to excellent carrier confinement, T_1 has values around 1800 K (from 20 to 70 °C), which means a very low η_d decrease: 0.0024 dB/°C. In turn, at high-CW drive levels, where ΔT_j reaches values in the 40–50 °C range,²³ P_{opt} decreases slightly. Thus, for relatively temperature-insensitive devices ΔT_j is mainly controlled by the R_{th} value. By contrast, devices with severe carrier leakage²⁴ have low- T_1 values [e.g., 140 K for the 0.99 μm emitting devices²⁴ of Ref. 20]. Then, if $T_1 = 140$ K and $\Delta T_j \approx 50$ K, the maximum obtainable P_{opt} and \bar{P}_{COMD} are at best 70% of the values for high- T_1 devices. In turn, \bar{P}_{COMD} in QCW operation becomes at least 85% higher than in CW operation, in good agreement with experiment.²⁰ Put a different way, for devices of low- R_{th} and $-R_s$ values (i.e., 2–3 mm long) \bar{P}_{COMD} in CW operation is a function of T_1 . For instance, for InGaAs-active devices, low- T_1 (140 K) 0.99 μm emitting lasers²⁰ have a CW \bar{P}_{COMD} of ~ 13 MW/cm², while high- T_1 (> 800 K) 0.92–0.98 μm emitting lasers^{4,25,26} have CW \bar{P}_{COMD} values in the 18–19 MW/cm² range. Similarly, 0.81 μm InGaAsP-active lasers²⁷ of low- T_1 value (260 K) have a CW \bar{P}_{COMD} of 13 MW/cm², while high- T_1 devices⁷ have a CW \bar{P}_{COMD} as high as 18 MW/cm².

The reason why \bar{P}_{COMD} is higher in QCW than in CW operation can be easily understood when considering that ΔT_j for 100 μs driven conventional devices is²⁸ $\sim 30\%$ of

ΔT_j in CW operation. In turn, the critical facet temperature rise ΔT_{cr} at which COMD is initiated²⁹ ($\Delta T_{\text{cr}} \sim 140$ K) in QCW operation is reached at higher power and drive levels than in CW operation.

In conclusion, the values of maximum CW power from diode lasers are primarily determined by four parameters: the equivalent spot size, d/Γ ; the power density at COMD, \bar{P}_{COMD} ; the temperature dependence of η_d ; and the heat removal ability of the heatsink.

The author gratefully acknowledges valuable technical discussions with D. Z. Garbuzov and L. J. Mawst as well as technical assistance from K. H. Ywn.

¹I. B. Petrescu-Prahova, M. Buda, and T. G. van de Roer, IEICE Trans. Electron. **E77-C**, 1472 (1994).

²D. Z. Garbuzov, J. H. Abeles, N. A. Morris, P. D. Gardner, A. R. Triano, M. G. Harvey, D. B. Gilbert, and J. C. Connolly, Proc. SPIE **2682**, 20 (1996).

³L. J. Mawst, A. Bhattacharya, J. Lopez, D. Botez, D. Z. Garbuzov, L. DeMarco, J. C. Connolly, M. Jansen, F. Fang, and R. F. Nabiev, Appl. Phys. Lett. **69**, 1532 (1996).

⁴A. Al-Muhanna, L. J. Mawst, D. Botez, D. Z. Garbuzov, R. U. Martinelli, and J. C. Connolly, Appl. Phys. Lett. **73**, 1182 (1998).

⁵N. Lichtenstein, R. Winterhoff, F. Scholz, and H. Schweizer, Tech. Dig. IEEE 16th International Semiconductor Laser Conference, Nara, Japan, 4–8 October 1998, p. 51.

⁶A. Knauer, G. Erbert, H. Wenzel, A. Bhattacharya, F. Bugge, J. Maegle, W. Pitroff, and J. Sebastian, Electron. Lett. **35**, 638 (1999).

⁷J. K. Wade, L. J. Mawst, D. Botez, and J. A. Morris, Electron. Lett. **34**, 1100 (1998).

⁸D. Garbuzov, R. Menna, R. Martinelli, J. Abeles, and J. Connolly, Electron. Lett. **33**, 1635 (1997).

⁹D. Garbuzov, R. Menna, H. Lee, R. U. Martinelli, J. C. Connolly, L. Xu, and S. R. Forrest, IEEE Proc. Conf. on InP and Related Compounds, Hyannis, MA, 11 May 1997, pp. 551–554.

¹⁰D. Botez, IEEE Conf. Proc. Lasers and Electro-Optics Society 1998 Ann. Mtg., Orlando, FL, 1–4 December 1998, pp. 274–275.

¹¹J. S. Yoo, H. H. Lee, and P. S. Zory, IEEE Photonics Technol. Lett. **3**, 594 (1991).

¹²R. Schatz and C. Bethea, J. Appl. Phys. **76**, 2509 (1994).

¹³D. Botez, RCA Rev. **39**, 577 (1978).

¹⁴D. Botez, IEEE J. Quantum Electron. **24**, 2034 (1988).

¹⁵D. Botez and M. Eitenberg, IEEE J. Quantum Electron. **QE-14**, 827 (1978).

¹⁶G. W. Yang, Z. T. Xu, X. Y. Ma, J. Y. Yu, J. M. Zhang, and L. H. Chen, Electron. Lett. **34**, 1312 (1998).

¹⁷G. Erbert, F. Bugge, A. Oster, J. Sebastian, R. Staske, K. Vogel, H. Wenzel, M. Weyers, and G. Traenkle, IEEE Conf. Proc. Lasers and Electro-Optics Society, 1997 Ann. Mtg., San Francisco, CA, 10–13 November 1997, pp. 199–200.

¹⁸A. Al-Muhanna, L. Mawst, D. Botez, D. Garbuzov, R. Martinelli, and J. Connolly, Appl. Phys. Lett. **71**, 1142 (1997).

¹⁹D. Z. Garbuzov, Tech. Dig. IEEE/OSA Conf. on Lasers and Electro-Optics '98, San Francisco, CA (1998), **6**, 10.

²⁰D. Z. Garbuzov, M. Gokhale, J. C. Dries, P. V. Studenkov, R. U. Martinelli, J. C. Connolly, and S. R. Forrest, Electron. Lett. **33**, 1462 (1997).

²¹D. P. Bour and A. Rosen, J. Appl. Phys. **66**, 2813 (1989).

²²L. J. Mawst, A. Bhattacharya, M. Nesnidal, J. Lopez, D. Botez, J. A. Morris, and P. Zory, Appl. Phys. Lett. **67**, 2901 (1995).

²³D. Z. Garbuzov (private communication).

²⁴M. Gokhale, J. C. Dries, P. V. Studenkov, S. R. Forrest, and D. Z. Garbuzov, IEEE J. Quantum Electron. **33**, 2266 (1997).

²⁵S. O'Brien, H. Zhao, A. Schoenfelder, and R. J. Lang, Electron. Lett. **33**, 1869 (1997).

²⁶X. He, S. Srinivasan, S. Wilson, C. Mitchell, and R. Patel, Electron. Lett. **34**, 2126 (1998).

²⁷G. Erbert, F. Bugge, A. Knauer, J. Maegle, A. Oster, J. Sebastian, R. Staske, and A. Thies, Proc. SPIE **3628**, 19 (1999).

²⁸M. Voss, C. Lier, V. Menzel, A. Barwolff, and T. Elsaesser, Tech. Dig. IEEE/OSA Conf. on Lasers and Electro-Optics '96, Anaheim, CA, **9**, 416.

²⁹P. W. Epperlein, Proc. SPIE **3001**, 13 (1997).